Label-free Tapered Fiber Optic Sensor for Real-time in Situ Detection of Cell Activity

Taiji Dong, Bingkun Gao, Bing Yan, Yekun Zhou, Yunkai Wang, Weicheng Wang, Kaichuan Xu, and Chunlei Jiang, Zengbo Wang.

***Abstract*—In the field of biomedicine, the non-destructive and label-free detection of individual living cells has been long pursued. We propose a tapered fiber optic biosensor (TFOB), and perform theoretical and simulation analyses of the optical intensity distribution of the fiber tip, which gradually becomes thinner to expose the evanescent field around it. The fiber tip becomes a highly sensitive sensing element that acts as a transduction mechanism for the evanescent field. It translates the intensity change of the evanescent field around the tapered fiber into changes in output power. Experimental results show that the developed TFOB can detect vibration signals with amplitudes as low as 3 nm and achieve nondestructive, label-free measurements of respiratory vibrations of pasta yeast cells. Results show the periodic motion of yeast cells in the range of 300–550 Hz. Meanwhile, inactivated yeast cells have no characteristic frequencies evident in the spectrum. This nanoscale fiber optic sensor offers potential technical support for cell activity detection and pathological analysis.**

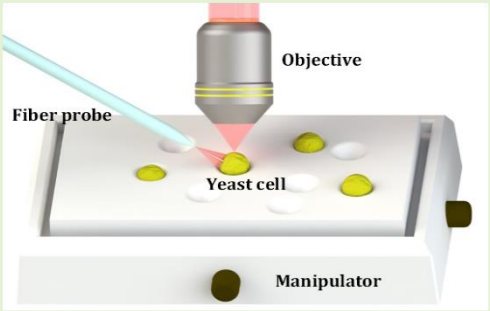

***Index Terms*—Microfiber, Optical fiber sensor, Cell activity assay, Optical interferometry**

I. INTRODUCTION

NANOSCALE vibrations of cell membranes or cell walls often play important roles when the human body is engaged in life activities such as protection of biomolecules, signaling, and exchange and transport of various substances [1-4]. A common feature of living organisms is movement, that is, even very small microorganisms vibrate as a result of their metabolic activity. As an important nanomechanical property of cell membranes or walls, nanoscale vibrations are closely related to biological metabolism and its life activities, and have become an important part of biomedicine and cell physiology [5-8].

The measurement and interpretation of the nanomechanical properties and local membrane motion of cells are often quite complex. Recent developments in nanotechnology have facilitated the development of nanoscale biosensors suitable for individual cell measurements. The detection of individual living cells in the living body can greatly improve our understanding of cellular function. In recent years, various chemical [9, 10], optical [1, 4], and mechanical methods [11, 12] with high accuracy and sensitivity have been developed to meet the needs of in vivo sample viability measurements [13]. Among nanomotor measurement methods, atomic force microscopy (AFM), a representative micro/nanomechanical oscillator sensor, has received a great deal of research attention [14, 15]. AFM has three main components, namely, the imaging part [16, 17], the force spectroscopy part [18], and the oscillation sensor part[19]; this method allows the imaging of individual membrane proteins or samples with nanoscale resolution in contrast to other microscopic imaging techniques. Currently, AFM oscillating cantilever technology has been widely used to monitor cell viability [14, 15, 20, 21], particularly in mitochondrial and ATP monitoring. Experimental results show that the amplitude difference is related to the state of mitochondria and their metabolic activity. However, this method ignores differences among individual cells. Although AFM single-cell force spectroscopy can be used to measure the adhesion of single cells, its productivity is not high in the determination of anticancer drugs and cell viability [22]. Moreover, the theoretical model cannot describe the change of cell shape caused by applying compression or shear force to the cell body due to the irregular shape of single cells; this limitation causes the method of calculating cell adhesion strength through surface stress very complex. In Ref. [23], the authors proposed a near-field optical device for detecting vibrations of living cells; the device uses a laser with a wavelength of 442 nm and a power of 200 mW as the

This work was supported by the Joint Guidance Project of Natural Science Foundation of Heilongjiang Province, China (LH2021F008). European Regional Development Fund (ERDF) and Welsh Government on Center for Photonics Expertise (CPE) Project, Grant Number: 81400. Special Funds for Higher Education Province (15011210803) (*Corresponding author: Chunlei Jiang, Zengbo Wang*)

Taiji Dong, Bingkun Gao, Yekun Zhou, Yunkai Wang, Weicheng Wang, Kaichuan Xu, and Chunlei Jiang. are with the School of Electrical Information Engineering, Northeast Petroleum University, Daqing 163000, China (e-mail: dongtaiji_nepu@126.com; gaobk@163.com; zyk9160@163.com; wangyunkai_nepu@163.com; wwc13473133327@163.com; jiangchunlei_nepu@163.com).

Kaichuan Xu is with the National Laboratory of Solid-State Microstructures and College of Engineering and Applied Sciences, Nanjing University, Jiangsu 210093, China (e-mail: xukaichuan_nepu@163.com).

Bing Yan, Zengbo Wang. are Department of Electrical Engineering, Bangor University (BGU), Bangor LL57 2DG, Britain (e-mail: b.yan@bangor.ac.uk; z.wang@bangor.ac.uk).

The authors declare no conflicts of interest.

illumination source. However, this method does not immobilize the cell under test, so determining whether the detected vibration comes from the cell itself is impossible. During the detection process of scanning near-field optical microscopy (SNOM), the undulation of a sample may block the detected light and cause the illusion of reduced amplitude because the spot is usually focused near the tip of the optical fiber close to the sample. In addition, the intensity of the laser light used to detect the probe vibration is stronger than the light entering the fiber from the aperture, thereby interfering with the near-field light signal detected by the probe aperture. In another example, detection with applied ultrasonic excitation obtains the vibrational frequency of a rigid cell motion by measuring the dynamic response of a single cell under ultrasonic basal excitation and relates it to the Young's modulus and surface tension of the cell through mathematical models [24]. However, this method cannot measure the respiratory motion of the cell itself; the ultrasound signal may interact with the sample and change the respiratory properties of the cell, affecting the measurement results. This problem is also present in the method for activity measurement of individual yeast cells proposed by Willaert *et al.* [25], the method is influenced by Brownian motion and background noise and does not directly measure the respiratory vibration of the cell wall.

As a dynamic organism, the cell's vibration varies with the metabolic cycle and in response to external stimuli. And the quantitative and dynamic observation of most cellular vibrations is still a gap. There is still a lack of a low-cost, convenient, and efficient method to detect weak nanoscale vibrations for in situ tracking of cellular vibrations.

In this study, we propose a tapered fiber optic biosensor (TFOB), which uses flame heating to stretch a single-mode fiber (SMF) so the cladding and core of the fiber become tapered. This progressively thinner fiber tip exposes the evanescent field to the surrounding area, thereby increasing the intensity and penetration depth of the evanescent field. In this case, the fiber tip becomes a highly sensitive sensing element. The fiber tip can emit light and act as a receiver, collecting feedback light from external objects for measurement. The high sensitivity and easy absorption of the evanescent field to increase the interaction between light and matter. In this regard, the field intensity distribution at the fiber tip is changed as the yeast cell approaches the tapered fiber tip. The respiratory vibration of the yeast cell can be measured in real time by monitoring changes in the light intensity signal output from the laser. The experiment results show that TFOB can effectively detect the respiratory vibration frequency of yeast cells, and can be used to distinguish between dead and highly active yeast cells.

II. Production and Principle

A. Fabrication of tapered fiber optic biosensor

Commercial SMF (Model: SMF-28e, connector type: FC/PC, core diameter: 8.2 μm, cladding diameter: 125 μm, NA=0.14) is used as raw material for fiber preparation. In the first step, the buffer layer and polymer protective jacket of the fiber are peeled off with a fiber stripper with a stripping length of 3 cm. The fiber is protected with a capillary tube (outer diameter ~1.1 mm, wall thickness ~0.1 mm, length ~100 mm) in protective jacket made of stainless steel to prevent fiber breakage and tangling. In the second step, the fiber is held in place by using grippers at both ends of the stepper motor. The fiber was heated with an alcohol lamp for about 5 seconds until it reaches its melting point. In the third step, the movement speed of the stepper motor is controlled to apply an initial pulling speed of 5 mm/s to the heated fiber, which reduces the fiber diameter from 125 μm to ~9 μm over a length of 2 cm, creating a progressively thinner taper. The speed of the stepper motor is then varied to form a region of abrupt thinning at a pulling speed of 20 mm/s. After the formation of the abrupt thinning region, the stretching of the fiber continues, after which the fiber is broken and the tip is thinned. The melted fibers form a tapered tip at the end under surface tension with a diameter of about 3.8 μm (the diameter of the yeast cells used in this study is about 5 μm). Finally, the stretched tip is wiped with a cleaning tissue moistened with alcohol, as is shown in Fig. 1(a), and the final TFOB is obtained.

B. The simulation of TFOB Light field distribution

Optical fiber is a concentric glass body composed of core and cladding, the core is generally composed of high-purity silica and dopants, which are used to increase the refractive index of the core, making the refractive index of the core n_1 higher than the refractive index of the cladding n_2, which ensures that the light in the fiber propagates forward in a total internal reflection manner. The light field in the fiber is mainly divided into two types, one is the light guide field in the fiber core, and the other is the exponentially decaying evanescent light field in the cladding, the expressions are as follows

$$E(x) = E_0 \exp\left(\frac{-x}{d_p}\right), \tag{1}$$

where x is the distance to the core, starting from $x = 0$ at the core-cladding interface, x_0 is the field strength at the interface, and d_p is the penetration depth.

The penetration depth d_p is indicated by [26]:

$$d_p = \frac{\lambda}{2\pi\sqrt{n_1^2 \sin^2\theta - n_2^2}}, \tag{2}$$

where λ is the wavelength of incident light, θ is the angle of incidence of light at the core/cladding interface, and n_1 and n_2 are the refractive indices (RI) of the fiber core and cladding, respectively.

In addition to the depth of penetration, the propagation of light in an optical fiber can be described in detail by using wave theory. The characteristics of the light in the fiber core are determined by the number of modes N. In the SMF, the light propagates in only one mode, but when the fiber undergoes deformation or the local refractive index changes, multiple modes are generated; coupling occurs among different modes, leading to an enhancement of the exposed evanescent field around the fiber tip; the increase in the evanescent field forms the basis for the increased sensitivity [26-28]. In this study, we fabricate the TFOB fiber, stretch the SMF by flame heating, and draw the cladding and core of the fiber into a tapered shape, which not only exposes the

evanescent field to the surrounding area but also increases the strength and penetration depth of the evanescent field. According to Ref. [29] the distal tapered region converts low-order modes to high-order modes, resulting in deeper and more efficient coupling in the cladding. In this case, the optical fiber tip becomes the sensing element, and the high sensitivity and easy absorption of the evanescent field are used to increase the interaction between light and matter, which in turn improves the sensitivity of the sensor. Moreover, the size of the tapered fiber is smaller than the cell diameter to ensure that the collected signal comes from the vibration of the yeast cell itself, which can effectively reduce the background signal during the measurement process.

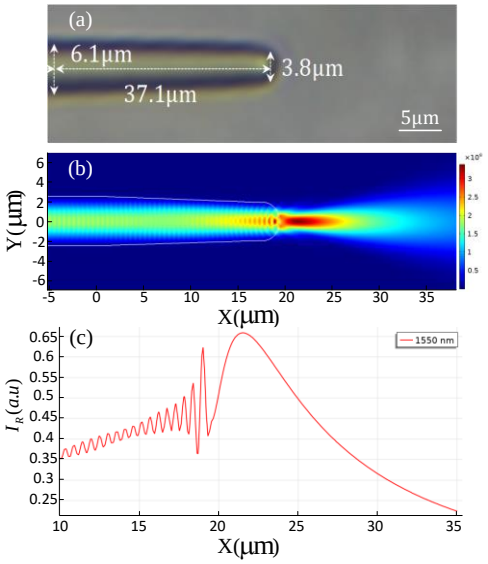

Fig.1. Schematic diagram of TFOB and optical field distribution at the fiber tip. (a) Optical microscope imaging of TFOB with tip diameter of 3.8 μm, scale bar, 5μm. (b) The output light field simulation results. (c) The light intensity distribution curve diagram.

To study the light intensity distribution at the tip of TFOB, we simulate the beam transmission of the fiber probe by using multi-physics software. Considering that the fiber optic probe used for particle capture is centrosymmetric, we simplify the model into two dimensions. All the simulation results are calculated in the XOY plane, which greatly reduces the computational effort. The parameters of the simulation are described as follows: the refractive index of the fiber and the refractive index of the solution are set to 1.46, and 1.3417 respectively; the wavelength of the incident light is 1550 nm; and the incident laser power is 1 W/m. The output light field simulation results are shown in Fig. 1(b). The light is focused near the fiber probe, and Fig. 1(c) shows the intensity of the light field as a function of distance.

III. Experiment and Results

A. PZT calibration experiment

To test the detection limit of the fabricated sensor, we select a piezoelectric transducer (PZT, P753.1CD, PI). The experiment setup is shown in Fig. 2, Distributed feedback laser (DFB, THORLABS, S3FC1550) is used as the laser source, the output power of the DFB is 2.0 mW, and a wavelength of 1550 nm. A 40-dB optical isolator has been packaged to eliminate frequency jitter due to back reflection, which could affect the measurement accuracy. Moreover, a reflector (R>0.9) is fixed to a PZT (P753.1CD, PI) as a vibrating target with a resolution of 0.05 nm under closed-loop control. PD is an invisible-light photodetector (PDA10CS-EC, Thorlabs). The light emitted from the DFB enters port 1 of the coupler and is divided into two beams by the coupler (50/50). One beam of light emitted from port 3 of the coupler enters the terminator to avoid interference with displacement signals. Another beam of light, which is emitted from port 4 of the coupler, enters the SMF after stretching and is used to detect the displacement of the PZT. The port 2 of the coupler is connected to the PD to collect the interference light. Signals are acquired by a data acquisition card (USB-4431, NI), which has a maximum sampling rate of 102.4 kHz. The signals are converted from analog into digital signal by the data acquisition card and then transmitted to the PC (Personal Computer) for subsequent data processing. The experimental equipment is placed on a precision optical bench (PTR52509, Thorlabs), which is equipped with four PTS602 active vibration isolation support legs for the experiments to avoid the effects of mechanical vibrations.

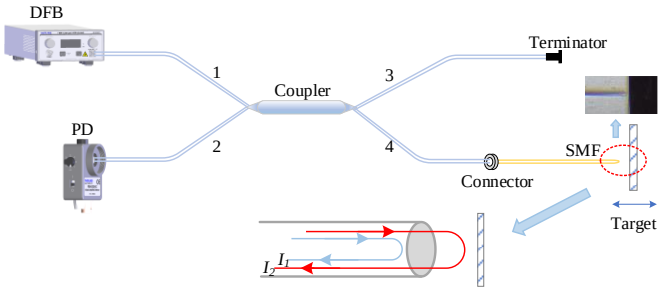

Fig.2. Experimental setup diagram of PZT calibration experiment.

To verify the reliability of this sensor, we carried out vibration measurements with larger than half wavelength. We set the amplitude of the PZT to 1 μm, and the detected waveform is shown in Fig. 3. Given that the amplitude is larger than half wavelength, the collected waveform contains a complete stripe, and each stripe represents half wavelength of displacement of the vibrating target.

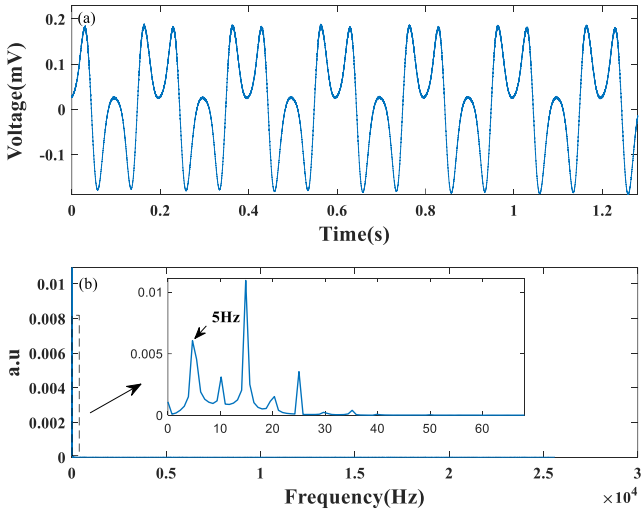

Fig.3. Experimental results of harmonic motion at 1 μm. (a) The F-P interference signal of 1 μm detected by PD. (b) The spectrum of the F-P interference signal.

Furthermore, we performed measurements at amplitude of 10, 8, 6, 4, and 3 nm. The experimental results in Fig. 4 show that the method can detect the vibration of 3 nm. According to Ref. [30], the yeast respiration for nanometer vibration can be used to verify, verifies the feasibility of the method for yeast vibration measurements.

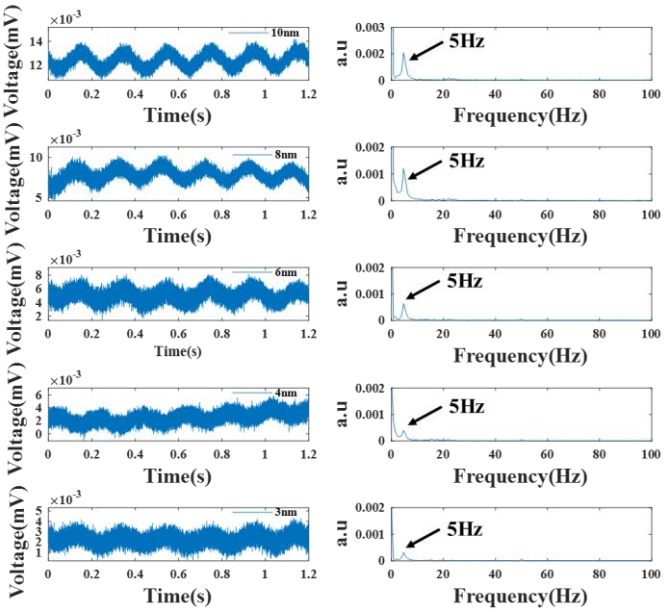

Fig. 4 The F-P interference signal and spectrum at the amplitude of 10, 8, 6, 4 and 3 nm, respectively.

B. Yeast cell vibration measurement

The device for measurement of yeast cell activity measurement device is shown in Fig. 5(a). The fiber probe is fixed to the manipulator and the position of the trapped yeast cells can be controlled by moving the specimen stage with the manipulator. Experimental images were acquired by an optical microscope through an integrated charge-coupled device (CCD). Images were observed and recorded on a computer in real-time. The laser, data acquisition card, and PD were kept to the same models as the above experiments. The household pasta yeast is chosen as the measurement object. Yeast cells were cultured using 5% glucose solution and incubated in a thermostat at 25°C for incubation. Immobilize round microbial cells, similar to yeast cells, on the surface of the culture medium is difficult; to address this problem, we used the same method as Ref. [30] to immobilize yeast by using a mechanical trapping technique. First, the yeast culture medium was filtered using a polycarbonate membrane, with a pore size of 5 μm, which acts as a mechanical trap. The filter was attached to the Petri dishes, and the surface was covered with YPD media. The dishes were placed in a thermostat and allowed to remain in thermal equilibrium for 1 hour. The cultured yeast solution was filtered with a 5 μm pore size polycarbonate membrane before and after filtration as shown in Fig. 5 (c) and Fig. 5 (d), respectively.

During the experiment, the position of the optical fiber probe was adjusted by three-axis manipulator to ensure that the yeast cells and the optical fiber probe were found in the imaging field at the same time. The fiber optic tip was kept at a certain distance (~200 nm) from the yeast cells by adjusting the micro-nano motion platform carrying the sample chamber. First, we selected yeast cells cultured for 24 hours as the experimental object, and the detection results are shown in Fig. 6. We selected different yeast cells for reproducibility measurements. The experimental results showed that the yeast cells had performing respiratory vibrations at a frequency of 549 Hz.

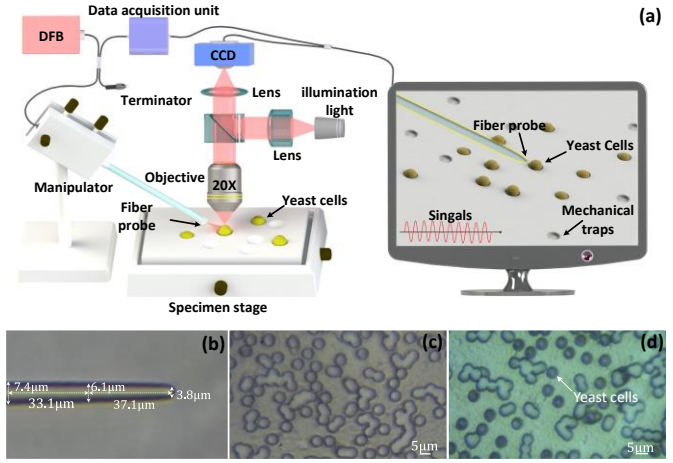

Fig.5. Nano vibration sensor cell detection and measurement results. (a) Experimental setup diagram of yeast cells vibration measurement. (b) The tip size of the stretched fiber probe is ~3.8 μm. (c) Diagram of polycarbonate membrane before filtration. (d) Diagram of the filtered polycarbonate membrane.

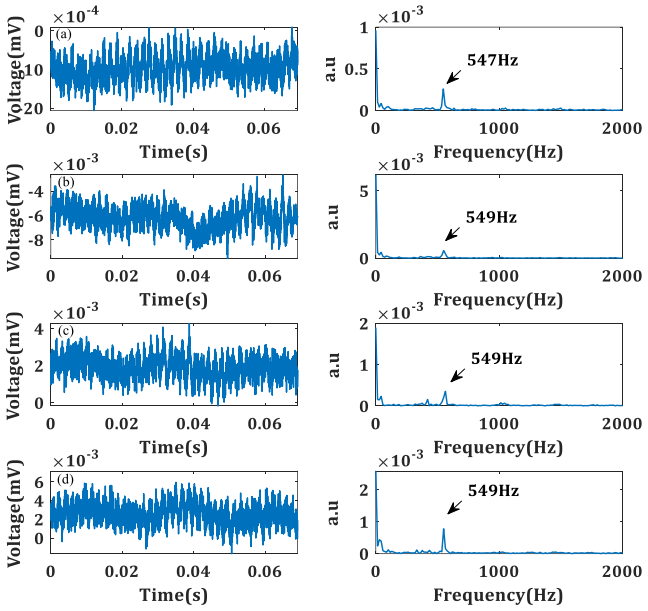

Fig.6. Typical time traces of respiratory vibrations of live yeast cells and frequency spectrogram.

To verify that the detected frequency is the vibration frequency of the yeast cell itself, we used 0.2% methylene blue solution for staining. The staining method mainly uses the integrity of the cell membrane and the metabolic ability of

metabolism to show cell activity. Live yeast cells have reductase, which reduces methylene blue to colorless. As shown in Fig. 7, when the yeast cells are immersed in methylene blue solution, the pigment enters the cells and is decolorized by the reductase. However, in dead cells, reductase is stained blue because it is inactivated and does not decolorize.

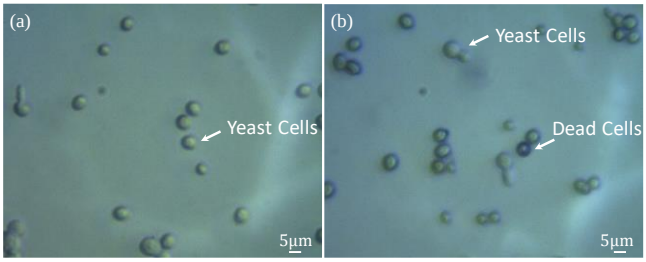

Fig.7. Schematic diagrams of mature yeast. (a) Mature yeast cells. (b) Yeast cells stained by methylene blue.

The stained and non-stained yeast cells was measured separately, and the results are shown in Fig. 8, the experimental results showed that the yeast cultured for 8 hours vibrated at ~430 Hz, while the yeast that had been inactivated could no longer detect any characteristic frequency in the spectrum.

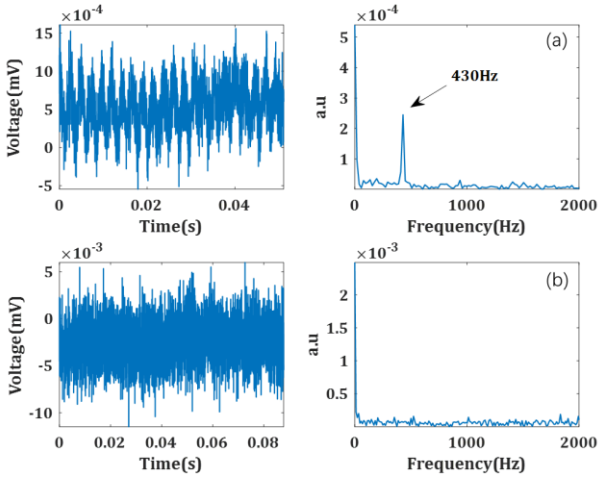

Fig.8. Yeast vibration signals. (a) Vibration signal and frequency spectrum of yeast cultured for 8 hours. (b) Vibration signal and spectrum of inactivated yeast.

Finally, we cultured the yeast cells in a thermostat at 25℃ for different periods and conducted vibration measurement tests. Furthermore, we performed repeatability measurements on different yeasts at the same cultivation time. We selected 10 yeast cells in the solution as and measured their activities after incubation for 2, 4, 8, and 24 hours. The experimental results are shown in Fig. 9. The activity of the yeast became stronger after prolonged incubation of 24 hours. In 2-4 hours, the vibration frequency of yeast cells did not increase significantly; at this time, the yeast cells are in the adjustment period to adapt to the new environment; temperature, pH, sugar, water, and so on changed, it is the activation process of metabolism. In 4-8 hours, the vibration frequency of yeast cells substantially increased; at this time, the yeast cells should be in the accelerated growth period. The yeast mainly carries out aerobic respiration, and cells proliferate in a logarithmic manner. In 8-24 hours, yeast cells are in the deceleration period of growth. The logarithmic growth period has a certain time limit due to various factors, such as drastically decreased content of fermentable sugars and oxygen, and increased alcohol and carbon dioxide. Moreover, the proliferation rate gradually decreases in the deceleration period. This finding indicates the feasibility of the method for cell vibration monitoring. The method provides a potential application for cell activity detection and even pathological analysis.

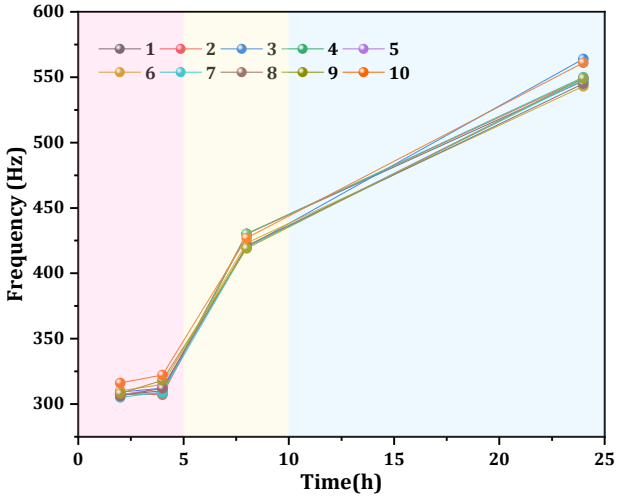

Fig.9. Results of the repeatability measurement.

IV. Conclusion

We propose a label-free, nondestructive reusable TFOB that enables real-time in situ measurements of cellular activity. This technology uses the sensitivity of nanomechanical sensors to translate the tiny motion characteristics of living systems. The intensity of such minute motions indicates the viability of the specimen and conveys information related to its metabolic activity. The developed technique can assess the viability of biological specimens. We applied the sensor to detect respiratory vibrations in yeast. The technique can successfully detect the characteristic frequencies of yeast respiration in the frequency spectrum. Furthermore, cellular activity was calibrated by methylene blue staining experiments and then probed using the optical fiber probe, which revealed significant differences in the spectrum between the dead yeast and the active yeast. The TFOB is easy to operate and has higher resolution than other biosensors. It is expected to be a perfect complement to traditional methods for biological cell detection. This nanoscale fiber optic sensor offers potential technical support for cell activity detection and even pathological analysis. For smaller cells or even subcellular structures, we can prepare finer TFOB probes to improve the resolution of the sensor. In future work, we consider combining TFOB with our previous work[31] to improve the sensitivity of the sensor and use it to evaluate single-cell activity with more quantitative metrics.

REFERENCES

[1] E. R. Kahle, N. Patel, H. B. Sreenivasappa *et al.*, "Targeting cell-matrix interface mechanobiology by integrating AFM with fluorescence microscopy," *Progress in Biophysics & Molecular Biology,* vol. 176, pp. 67-81, Dec, 2022.

[2] J. L. Shi, L. Q. Liu, P. Yu *et al.*, "Real-time detecting and tracking nanoscale feeble vibrations based SF-AM AFM," *IEEE International Conference on Intelligent Robots and Systems.* pp. 1976-1981, 2015.

[3] A. Lostao, K. Lim, M. C. Pallares *et al.*, "Recent advances in sensing the inter-biomolecular interactions at the nanoscale - A comprehensive review of AFM-based force spectroscopy," *International journal of biological macromolecules,* vol. 238, pp. 124089, 2023 Mar 21 (Epub 2023 Mar, 2023.

[4] Y. F. Dufrene, A. Viljoen, J. Mignolet *et al.*, "AFM in cellular and molecular microbiology," *Cellular Microbiology,* vol. 23, no. 7, pp. 12, Jul, 2021.

[5] P. G. Childs, C. A. Boyle, G. D. Pemberton *et al.*, "Use of nanoscale mechanical stimulation for control and manipulation of cell behaviour," *Acta Biomaterialia,* vol. 34, pp. 159-168, Apr, 2016.

[6] Z. Nix, D. Kota, I. Ratnayake *et al.*, "Spectral characterization of cell surface motion for mechanistic investigations of cellular mechanobiology," *Progress in Biophysics & Molecular Biology,* vol. 176, pp. 3-15, Dec, 2022.

[7] V. S. Chaudhary, D. Kumar, and S. Kumar, "Gold-immobilized photonic crystal fiber-based SPR biosensor for detection of malaria disease in human body," *IEEE Sensors Journal,* vol. 21, no. 16, pp. 17800-17807, 2021.

[8] V. S. Chaudhary, D. Kumar, G. P. Mishra *et al.*, "Plasmonic biosensor with gold and titanium dioxide immobilized on photonic crystal fiber for blood composition detection," *IEEE Sensors Journal,* vol. 22, no. 9, pp. 8474-8481, 2022.

[9] L. D. Yu, N. Li, Y. J. Tong *et al.*, "From exogenous to endogenous: Advances in in vivo sampling in living systems," *Trac-Trends in Analytical Chemistry,* vol. 156, pp. 10, Nov, 2022.

[10] F. G. Fan, C. Y. Xu, X. A. Liu *et al.*, "A novel ESIPT-based fluorescent probe with dual recognition sites for the detection of hydrazine in the environmental water samples and in-vivo bioimaging," *Spectrochimica Acta Part a-Molecular and Biomolecular Spectroscopy,* vol. 280, pp. 8, Nov, 2022.

[11] J. Hu, X. P. Li, R. L. Judd *et al.*, "Rapid lipolytic oscillations in ex vivo adipose tissue explants revealed through microfluidic droplet sampling at high temporal resolution," *Lab on a Chip,* vol. 20, no. 8, pp. 1503-1512, Apr, 2020.

[12] I. H. Faris, J. Melchor, A. Callejas *et al.*, "Viscoelastic Biomarkers of Ex Vivo Liver Samples via Torsional Wave Elastography," *Diagnostics,* vol. 10, no. 2, pp. 18, Feb, 2020.

[13] M. Wei, R. Zhang, F. Zhang *et al.*, "Evaluating cell viability heterogeneity based on information fusion of multiple adhesion strengths," *Biotechnology and Bioengineering,* vol. 118, no. 6, pp. 2360-2367, Jun, 2021.

[14] F. S. Ruggeri, A.-L. Mahul-Mellier, S. Kasas *et al.*, "Amyloid single-cell cytotoxicity assays by nanomotion detection," *Cell Death Discovery,* vol. 3, 2017, 2017.

[15] T. Vannocci, S. Dinarelli, M. Girasole *et al.*, "A new tool to determine the cellular metabolic landscape: nanotechnology to the study of Friedreich's ataxia," *Scientific Reports,* vol. 9, Dec 17, 2019.

[16] F. Z. Xia, and K. Youcef-Toumi, "Review: Advanced Atomic Force Microscopy Modes for Biomedical Research," *Biosensors-Basel,* vol. 12, no. 12, pp. 24, Dec, 2022.

[17] Y. X. Zhou, and J. Du, "Atomic force microscopy (AFM) and its applications to bone-related research," *Progress in Biophysics & Molecular Biology,* vol. 176, pp. 52-66, Dec, 2022.

[18] L. T. Liu, M. S. Du, and F. Liu, "Recent advances in interface microscopic characterization of carbon fiber-reinforced polymer composites," *Frontiers in Materials,* vol. 10, pp. 18, Feb, 2023.

[19] H. Yabuno, "Review of applications of self-excited oscillations to highly sensitive vibrational sensors," *Zamm-Zeitschrift Fur Angewandte Mathematik Und Mechanik,* vol. 101, no. 7, pp. 13, Jul, 2021.

[20] S. Kasas, F. S. Ruggeri, C. Benadiba *et al.*, "Detecting nanoscale vibrations as signature of life," *Proceedings of the National Academy of Sciences of the United States of America,* vol. 112, no. 2, pp. 378-381, Jan 13, 2015.

[21] Y. Fang, R. Riedel, P. del Pino *et al.*, "Real-time, label-free monitoring of cell viability based on cell adhesion measurements with an atomic force microscope," *Journal of Nanobiotechnology,* vol. 15, Mar 22, 2017.

[22] H. Al-Madani, H. Du, J. Yao *et al.*, "Living Sample Viability Measurement Methods from Traditional Assays to Nanomotion," *Biosensors-Basel,* vol. 12, no. 7, Jul, 2022.

[23] R. Piga, R. Micheletto, and Y. Kawakami, "Acoustical nanometre-scale vibrations of live cells detected by a near-field optical setup," *Optics Express,* vol. 15, no. 9, pp. 5589-5594, Apr, 2007.

[24] B. Farzi, and C. Cetinkaya, "Micromechanical and surface adhesive properties of single saccharomyces cerevisiae cells," *Journal of Physics D-Applied Physics,* vol. 50, no. 37, pp. 11, Sep, 2017.

[25] R. G. Willaert, P. Vanden Boer, A. Malovichko *et al.*, "Single yeast cell nanomotions correlate with cellular activity," *Sci Adv,* vol. 6, no. 26, pp. eaba3139, Jun, 2020.

[26] A. Leung, P. M. Shankar, and R. Mutharasan, "A review of fiber-optic biosensors," *Sensors and Actuators B-Chemical,* vol. 125, no. 2, pp. 688-703, Aug, 2007.

[27] N. Díaz-Herrera, M. C. Navarrete, O. Esteban *et al.*, "A fibre-optic temperature sensor based on the deposition of a thermochromic material on an adiabatic taper," *Measurement Science and Technology,* vol. 15, no. 2, pp. 353-358, 2004.

[28] A. G. Mignani, R. Falciai, and L. Ciaccheri, "Evanescent wave absorption spectroscopy by means of bi-tapered multimode optical fibers," *Applied Spectroscopy,* vol. 52, no. 4, pp. 546-551, Apr, 1998.

[29] G. Y. Chen, "Profile optimization of tapered waveguide sensors by fluorescence imaging," *Proceedings of SPIE.* pp. 70-77, 2004.

[30] A. E. Pelling, S. Sehati, E. B. Gralla *et al.*, "Local nanomechanical motion of the cell wall of Saccharomyces cerevisiae," *Science,* vol. 305, no. 5687, pp. 1147-1150, Aug, 2004.

[31] W. Wang, C. Jiang, S. Tian *et al.*, "Microsphere-assisted Fabry–Perot interferometry: proof of concept," *Applied Optics,* vol. 61, no. 18, 2022.